

Single-Crystal Reflectance Studies of Tetrathiafulvalene Tetracyanoquinodimethane*

C. S. Jacobsen,† D. B. Tanner,‡ A. F. Garito, and A. J. Heeger
*Department of Physics and Laboratory for Research on the Structure of Matter,
 University of Pennsylvania, Philadelphia, Pennsylvania 19174*

(Received 14 October 1974)

The polarized reflectance of single crystals of tetrathiafulvalene tetracyanoquinodimethane (TTF-TCNQ) at 300 K is reported over the frequency range 300 to 4000 cm^{-1} , with unpolarized data extending to 50 cm^{-1} . A Kramers-Kronig analysis is used to obtain the frequency-dependent conductivity $\sigma_1(\omega)$ and dielectric function, $\epsilon_1(\omega)$, for both a and b crystallographic axes. The results establish the existence of the energy gap and provide a quantitative measurement of the oscillator strength and relaxation time of the collective mode.

The existence of a gap¹ in the electronic excitation spectrum of tetrathiafulvalene-tetracyanoquinodimethane (TTF-TCNQ) is of central importance to understanding the origin of the remarkable transport properties of this organic metal.²⁻⁶ The energy gap in the infrared ($E_g \approx 0.14$ eV) together with the relatively large dc²⁻⁴ and microwave⁶ conductivities imply a correlated many-body state in which the low-frequency conductivity results from a collective mode. We report single-crystal reflectivity measurements in the range from 50 through 4000 cm^{-1} . The results confirm the energy gap as obtained from earlier work on thin films,¹ and place a lower limit on the collective-mode lifetime.

The infrared (ir) reflectivity measurements were performed on single crystals ca. 2×10 mm² using as-grown surfaces.⁷ ir spectra were recorded using a Perkin-Elmer 225 spectrophotometer over the region 300 to 4000 cm^{-1} , and a Grubb-Parsons Michelson interferometer in the range from 50 to 500 cm^{-1} . Figure 1 shows the polarized reflectance at room temperature for $E \parallel b$ and $E \parallel a$ in the range 300–4000 cm^{-1} . The dashed lines from 50 to 300 cm^{-1} were obtained from unpolarized reflectance from carefully aligned single crystals; $R(E \parallel b)$ was calculated by assuming that $R(E \parallel a)$ is constant at the 300- cm^{-1} value, so that $R(E \parallel b) = 2R_{\text{unpolarized}} - R(E \parallel a)$. Throughout the ir, $R(E \parallel a)$ is essentially frequency independent except for several sharp structures arising from intramolecular vibrations.

Over the intermediate ir, $R(E \parallel b)$ has values of less than 72%, i.e., considerably below the values that would be expected from a simple metal with a dc conductivity²⁻⁴ between 500–1000 ($\Omega \text{ cm}$)⁻¹ and a plasma edge at 7000 cm^{-1} .⁸⁻¹¹ The relatively low reflectance at long wavelengths implies an energy gap $E_g = \hbar\omega_g$ with $\omega_g\tau_{sp} \sim 1$,

where τ_{sp} is the single-particle scattering time appropriate to excitations near the gap edge.

Since the polarized reflectance is known for frequencies up to 37000 cm^{-1} ,⁸⁻¹⁰ a Kramers-Kronig analysis is expected to give reliable results in the ir. This procedure consists of calculating the phase shift $\theta(\omega)$ from the dispersion relation:

$$\theta(\omega) = \frac{\omega}{\pi} P \int_0^{\infty} \frac{\ln R(\omega') - \ln R(\omega)}{\omega'^2 - \omega^2} d\omega'. \quad (1)$$

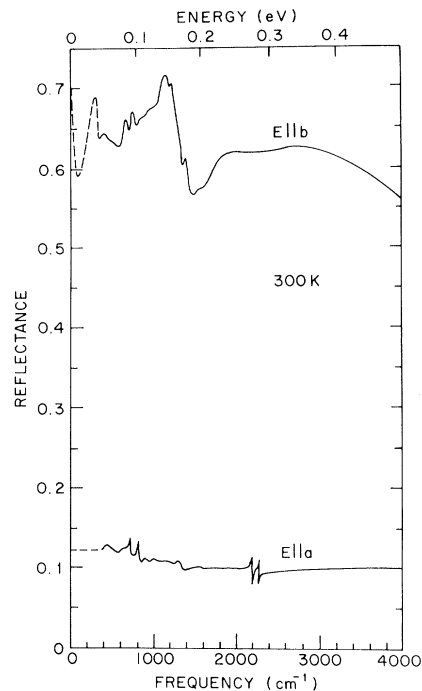


FIG. 1. Single-crystal reflectance of TTF-TCNQ. The curves labeled $E \parallel b$ and $E \parallel a$ represent polarized reflectance data with electric field vector parallel to the crystallographic b and a axes, respectively.

The complex index of refraction is then obtained from the inverted Fresnel formula

$$N = n + ik = [\epsilon_1 + i(4\pi/\omega)\sigma_1]^{1/2} \\ = (1 + R^{1/2}e^{i\theta}) / (1 - R^{1/2}e^{i\theta}). \quad (2)$$

Since $R(\omega)$ is known for $50 < \omega < 37\,000 \text{ cm}^{-1}$, conventional extrapolation procedures were employed.¹² In the range $0 < \omega < 50 \text{ cm}^{-1}$, it was assumed that $R(E \parallel b)$ behaves according to the Hagen-Rubens formula, $R = 1 - A\omega^{1/2}$, with the parameter A chosen so that a smooth connection with the data was obtained. The value for $R(E \parallel a)$ was assumed constant in this range. The high-frequency extrapolation must simulate interband and (at very high frequencies) free-electron behavior. For the b -axis data we have used the standard approximation, $R(\omega) = R(\omega_c)(\omega_c/\omega)^P$, with $\omega_{c1} = 37\,000 \text{ cm}^{-1}$, $P_1 = 2$ (corresponding to interband transitions), and with $\omega_{c2} = 2 \times 10^5 \text{ cm}^{-1}$, $P_2 = 4$ (corresponding to free-electron behavior).

The frequency-dependent conductivity $\sigma_1(\omega)$ and dielectric function $\epsilon_1(\omega)$, as obtained from the Kramers-Kronig analysis, are shown for $E \parallel b$ and $E \parallel a$ in Figs. 2 and 3.

The insensitivity to the extrapolation procedures is illustrated by the following examples.

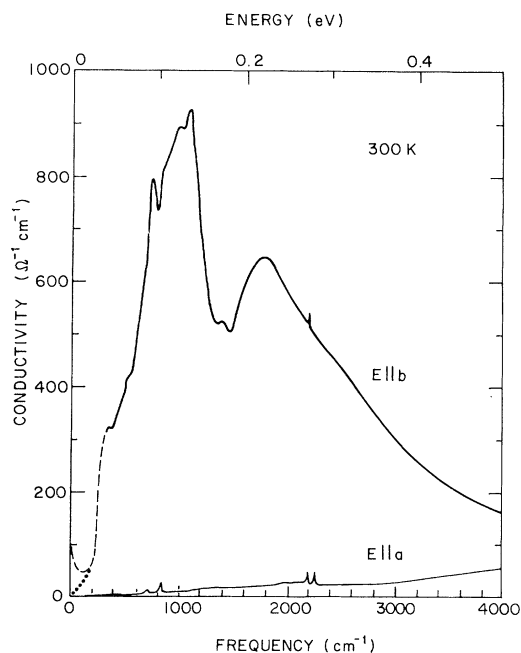


FIG. 2. The frequency-dependent conductivities $\sigma_1^b(\omega)$ and $\sigma_1^a(\omega)$ as obtained from Kramers-Kronig analysis. The dotted and dashed curves below 200 cm^{-1} represent two different low-frequency extrapolations (see text).

Assuming $R(E \parallel b)$ constant for $\omega < 50 \text{ cm}^{-1}$ leads to changes in σ_1 less than 2% for $\omega > 500 \text{ cm}^{-1}$, and gives in the gap region even lower values for σ_1 (the dotted curve below 200 cm^{-1}) than the Hagen-Rubens extrapolation (the dashed curve below 200 cm^{-1}). Assuming constant reflectance above $37\,000 \text{ cm}^{-1}$ changes $\sigma_1^b(\omega)$ less than 10% for any $\omega < 10^4 \text{ cm}^{-1}$, and has negligible effect below 500 cm^{-1} .

The main features in $\sigma_1^b(\omega)$ are a resonant structure with an absolute maximum at approximately 1100 cm^{-1} with a relatively narrow minimum centered at approximately 1400 cm^{-1} . At higher frequencies a smooth, Drude-like frequency dependence is observed. The general shape and detailed structure are in excellent agreement with the thin-film data.¹ The larger peak value and narrower width of the single-crystal $\sigma_1^b(\omega)$ imply a longer single-particle scattering time, as expected.^{8,9}

The corresponding behavior of $\epsilon_1^b(\omega)$ (Fig. 3) is that of an insulator with a transition across the energy gap sufficiently strong to give negative values between 1000 and 6000 cm^{-1} . At lower frequencies, ϵ_1^b is positive with a maximum of 82 near 300 cm^{-1} , while the detailed behavior in the far ir is not known. The general shape

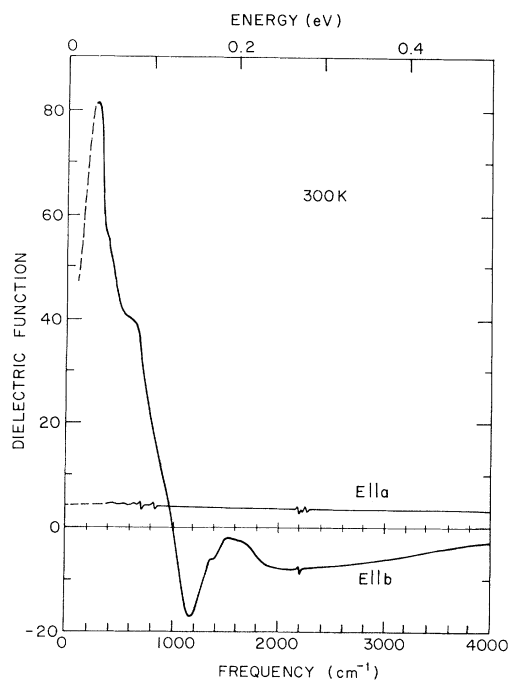


FIG. 3. The frequency-dependent dielectric functions $\epsilon_1^b(\omega)$ and $\epsilon_1^a(\omega)$ as obtained from Kramers-Kronig analysis.

and detailed structure are once again in excellent agreement with the thin-film data.¹

The single-crystal reflectivity results thus establish the existence of the energy gap in the excitation spectrum. The gap is well defined even at room temperature where fluctuation effects would suggest a relatively high density of states in the gap region.¹³ That there are states in the gap can be inferred from the magnetic susceptibility.¹⁴⁻¹⁶ The susceptibility shows the qualitative features predicted by Lee, Rice, and Anderson,¹³ and would imply that at room temperature the density of states near E_F is within 20% of the unperturbed value. In contrast, $\sigma_1^b(\omega)$ in the gap region below 400 cm^{-1} is more than an order of magnitude below the gapless Drude curve. We infer that the pseudogap in $\sigma_1(\omega)$ is in essence a mobility gap¹⁷ caused by the strong dynamic fluctuations in local potential due to the inherent fluctuations in the one-dimensional system.

The *single-crystal* results for the frequency-dependent b -axis conductivity can thus be summarized as follows: (i) Zero frequency (dc): The conductivity is approximately $10^3 (\Omega \text{ cm})^{-1}$ at room temperature, increasing to values exceeding 10^4 – $10^5 (\Omega \text{ cm})^{-1}$ near 58 K.²⁻⁴ (ii) Microwave frequency (10^{10} GHz): The conductivity is approximately $10^3 (\Omega \text{ cm})^{-1}$ at room temperature, increasing to values exceeding $10^4 (\Omega \text{ cm})^{-1}$ near 58 K.⁶ At both dc and microwave frequencies it appears likely that the peak conductivities are defect limited. (iii) Infrared frequencies: There is an energy gap¹ with magnitude $\hbar\omega_g \approx 0.14 \text{ eV}$ above which the single-particle conductivity is Drude-like with a plasma frequency⁸⁻¹¹ of $\hbar\omega_p \approx 1.2 \text{ eV}$.

These results are sketched in Fig. 4, which is drawn to describe qualitatively the frequency dependence of $\sigma_1(\omega)$ near 60 K using typical values.

The collective-mode lifetime τ_c has not yet been measured directly. However, this width can be estimated from the collective-mode oscillator strength Ω_p^2 and the measured dc conductivity, since¹⁸ $\sigma_{\text{collective}} = (4\pi)^{-1} \Omega_p^2 \tau_c$. An upper limit to Ω_p^2 can be inferred from the single-crystal data. Since the width is less than the lowest measuring frequency, $\epsilon_1 = 100 - \Omega_p^2/\omega^2$. $\Re(E \parallel b)$ remains nearly constant at approximately 70% and does not begin to rise toward unity even in the range 50 to 100 cm^{-1} . Thus, we can conservatively construct the inequality $\Omega_p^2 < 10^6 \text{ cm}^{-2}$ [a rapid rise toward $\Re(E \parallel b) \sim 1$ is required when $\epsilon_1 < 0$]. Using $\sigma_{\text{dc}}(300 \text{ K}) = 10^3 (\Omega \text{ cm})^{-1}$ leads to $\tau_c^{-1}(300 \text{ K}) < 3 \times 10^{12} \text{ sec}^{-1}$ (16 cm^{-1}). Assuming

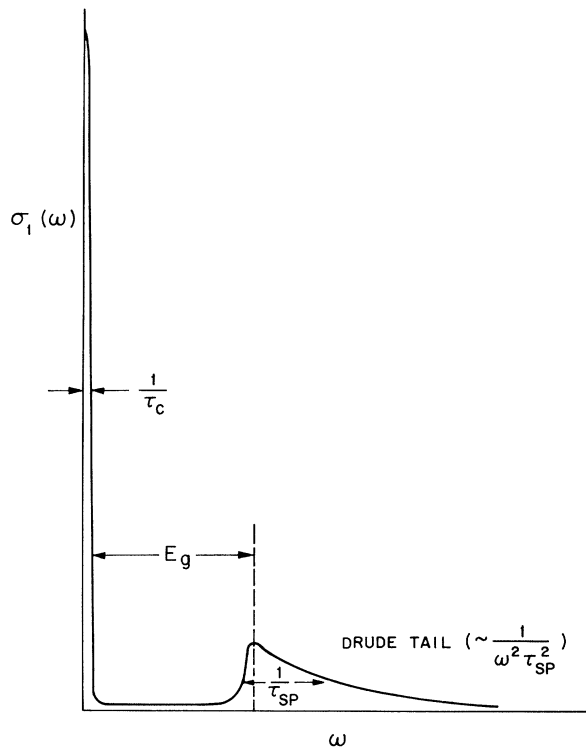


FIG. 4. Schematic diagram of $\sigma_1^b(\omega)$ for TTF-TCNQ as obtained from single-crystal data (see text). The curve is drawn using a typical value of $2 \times 10^4 (\Omega \text{ cm})^{-1}$ for the dc conductivity.

conservation of oscillator strength with decreasing temperature, a peak conductivity near 60 K in the range of 10^4 – $10^5 (\Omega \text{ cm})^{-1}$ implies $\tau_c^{-1}(60 \text{ K}) \sim 10^{11} \text{ sec}^{-1}$ ($\sim 0.5 \text{ cm}^{-1}$). Thus the collective-mode lifetime is enhanced over the single-particle scattering time by at least 2 orders of magnitude at room temperature and more than 3 orders of magnitude near 60 K. This comparison represents one of the clearest indications of coherence in the “metallic” state of TTF-TCNQ.

Much of the discussion surrounding the study of TTF-TCNQ and related systems centered on the dc electrical conductivity. However, it is now generally agreed that the intrinsic conductivity exceeds $10^4 (\Omega \text{ cm})^{-1}$ and there is evidence that the peak value exceeds $10^5 (\Omega \text{ cm})^{-1}$.⁴ The sensitivity of the one-dimensional conductor to impurities and defects has been established,^{4,6} so that these values may only be lower bounds. However, it is most important to view the dc and microwave conductivities in the context of the overall experimental knowledge of $\sigma_1(\omega)$ and $\epsilon_1(\omega)$ as obtained from single-crystal data and the earlier work on thin films.¹ TTF-TCNQ is not a

simple metal; it has the optical spectrum of a semiconductor, but conducts at zero frequency because of a long-lifetime collective mode.

*Work supported by the National Science Foundation through the Laboratory for Research on the Structure of Matter and Grant No. GH-39303, and by the Advanced Research Projects Agency through Grant No. DAHC 15-72C-0174.

†Present address: Physics Laboratorium III, The Technical University of Denmark, DK-2800 Lyngby, Denmark.

‡Present address: Physics Department, Ohio State University, Columbus, Ohio 43210.

¹D. B. Tanner, C. S. Jacobsen, A. F. Garito, and A. J. Heeger, *Phys. Rev. Lett.* **32**, 1301 (1974).

²L. B. Coleman, M. J. Cohen, D. J. Sandman, F. G. Yamagishi, A. F. Garito, and A. J. Heeger, *Solid State Commun.* **12**, 1125 (1973).

³J. Ferraris, D. O. Cowan, V. Walatka, Jr., and J. H. Perlstein, *J. Amer. Chem. Soc.* **95**, 948 (1973).

⁴M. J. Cohen, L. B. Coleman, A. F. Garito, and A. J. Heeger, *Phys. Rev. B* **10**, 1298 (1974).

⁵P. M. Chaikin, J. F. Kwak, T. E. Jones, A. F. Garito, and A. J. Heeger, *Phys. Rev. Lett.* **31**, 601 (1973); J. F. Kwak, P. M. Chaikin, A. A. Russel, A. F. Garito, and A. J. Heeger, to be published.

⁶S. K. Khanna, E. Ehrenfreund, A. F. Garito, and A. J. Heeger, *Phys. Rev. B* **10**, 2205 (1974).

⁷These were all TTF-TCNQ(D₈); the deuterated material grew into relatively large single crystals suitable for the infrared measurements.

⁸A. A. Bright, A. F. Garito, and A. J. Heeger, *Solid State Commun.* **13**, 943 (1974).

⁹A. A. Bright, A. F. Garito, and A. J. Heeger, *Phys. Rev. B* **10**, 1328 (1974).

¹⁰P. M. Grant, R. L. Greene, G. C. Wrighton, and G. Castro, *Phys. Rev. Lett.* **31**, 1311 (1973).

¹¹P. I. Perov and J. Fischer, *Phys. Rev. Lett.* **33**, 521 (1974).

¹²See, for example, F. Wooten, *Optical Properties of Solids* (Academic, New York, 1972), p. 248.

¹³P. A. Lee, T. M. Rice, and P. W. Anderson, *Phys. Rev. Lett.* **31**, 462 (1973).

¹⁴J. C. Scott, A. F. Garito, and A. J. Heeger, *Phys. Rev. B* (to be published).

¹⁵J. H. Perlstein, J. P. Ferraris, V. V. Walatka, D. O. Cowan, and G. A. Candela, in *Magnetism and Magnetic Materials—1972*, AIP Conference Proceedings No. 10, edited by C. D. Graham, Jr., and J. J. Rhyne (American Institute of Physics, New York, 1973), p. 1494.

¹⁶Y. Tomkiewicz, B. A. Scott, L. J. Tao, and R. S. Title, *Phys. Rev. Lett.* **32**, 1363 (1974).

¹⁷A similar analysis leading to the inference of a mobility gap in K₂[Pt(CN)₄]Cl_{0.3}·3H₂O (KCP) has been presented by H. R. Zeller (private communication).

¹⁸M. J. Rice, S. Strässler, and W. R. Schneider, in "Saarbrücken Conference on One-Dimensional Conductors," Saarbrücken, Germany, June 1974, edited by H. G. Schuster (Springer, Berlin, to be published).

From Giant Moment to Kondo and Spin Glass Behavior: The Electrical Resistivity of PdFe and (PdFe)H

J. A. Mydosh

Institut für Festkörperforschung der Kernforschungsanlage, D-517 Jülich, Germany
(Received 1 October 1974)

I have measured the low-temperature electrical resistivity $\rho(T)$ for a series of PdFe alloys with and without hydrogenation. For Pd+0.2 at.% Fe, the sharp decrease in $\rho(T)$ at the Curie temperature gives way to a broad Kondo-like minimum. With increasing Fe concentration, the giant-moment ferromagnetism is severely hindered by hydrogen charging, and $\rho(T)$ shows the characteristics of an interacting Kondo system or a "spin glass."

Palladium-iron is a well-known giant-moment system which orders ferromagnetically with small amounts of iron ($c \approx 0.1$ at.% Fe).¹⁻³ On the other hand, elemental Pd can be easily charged with large amounts of hydrogen and becomes superconducting for H/Pd ≈ 0.75 .^{4,5} It has further been established that the large exchange-enhanced Pauli paramagnetic susceptibility of Pd linearly decreases with hydrogenation, and at H/Pd ≈ 0.65 a slightly negative or diamagnetic susceptibility

is found.⁶ Recent theories^{7,8} have considered this result as a necessary (but not sufficient) condition for the rather high superconducting transition temperature (≈ 9 K) of palladium hydride.⁵

As the exchange enhancement of Pd and the giant moments of PdFe lead to large effects in the electrical resistivity,^{9,10} any modification of the Pd matrix polarizability should be strongly reflected in $\rho(T)$ and $d\rho(T)/dT$. Furthermore, the hydrogenation of PdFe is especially signifi-